

GSA DATA REPOSITORY 2016242

Synchronous diversification of Laurentian and Baltic rhynchonelliform brachiopods:

Implications for regional versus global triggers of the Great Ordovician Biodiversification Event

Sarah Trubovitz and Alycia L. Stigall

doi:10.1130/G38083.1

Part 1: Stratigraphic data

Sampling locations

In total, 426 of the 655 meters of the Simpson Group were exposed along I-35. The lower Joins Formation was measured at 34°21'54.55''N 97°8'47.04'' W. The upper Joins Formation was measured at 34°21'47.84''N 97°8'27.76''W. The Oil Creek Formation was measured at 34°21'53.98''N 97° 8'47.23''W. The McLish Formation was measured at 34°26'10.64''N 97° 7'42.46''W. The lower Tulip Creek Formation was measured at 34°26'14.79''N 97°7'42.09''W. The upper Tulip Creek Formation was measured at 34°21'29.89''N 8'39.61''W. The Mountain Lake Member of the Bromide Formation was measured at 34°26'7.67''N 97°7'45.65''W and 34°24'17.53''N 96°57'1.91''W. Complete stratigraphic columns and brachiopod diversity data are available in Trubovitz (2016). Missing section included most of the Joins Formation, uppermost Oil Creek Formation, uppermost McLish Formation, most of the non-sandstone portions of the Tulip Creek Formation, and the basal Bromide Formation as indicated in Figure DR1. These sections are not exposed in the study region due to a combination of tectonic and weathering processes.

Correlation and age model

Measured sections were correlated with published North American midcontinent conodont zones (Bauer, 1987, 1994, 2010), enabling comparison to the North Atlantic conodont zones and graptolite zones used to constrain brachiopod diversity on other paleocontinents

(based on Cooper and Sadler, 2012). Notably, the sections measured for this study are the same as those examined by (Bauer, 1987, 1994, 2010).

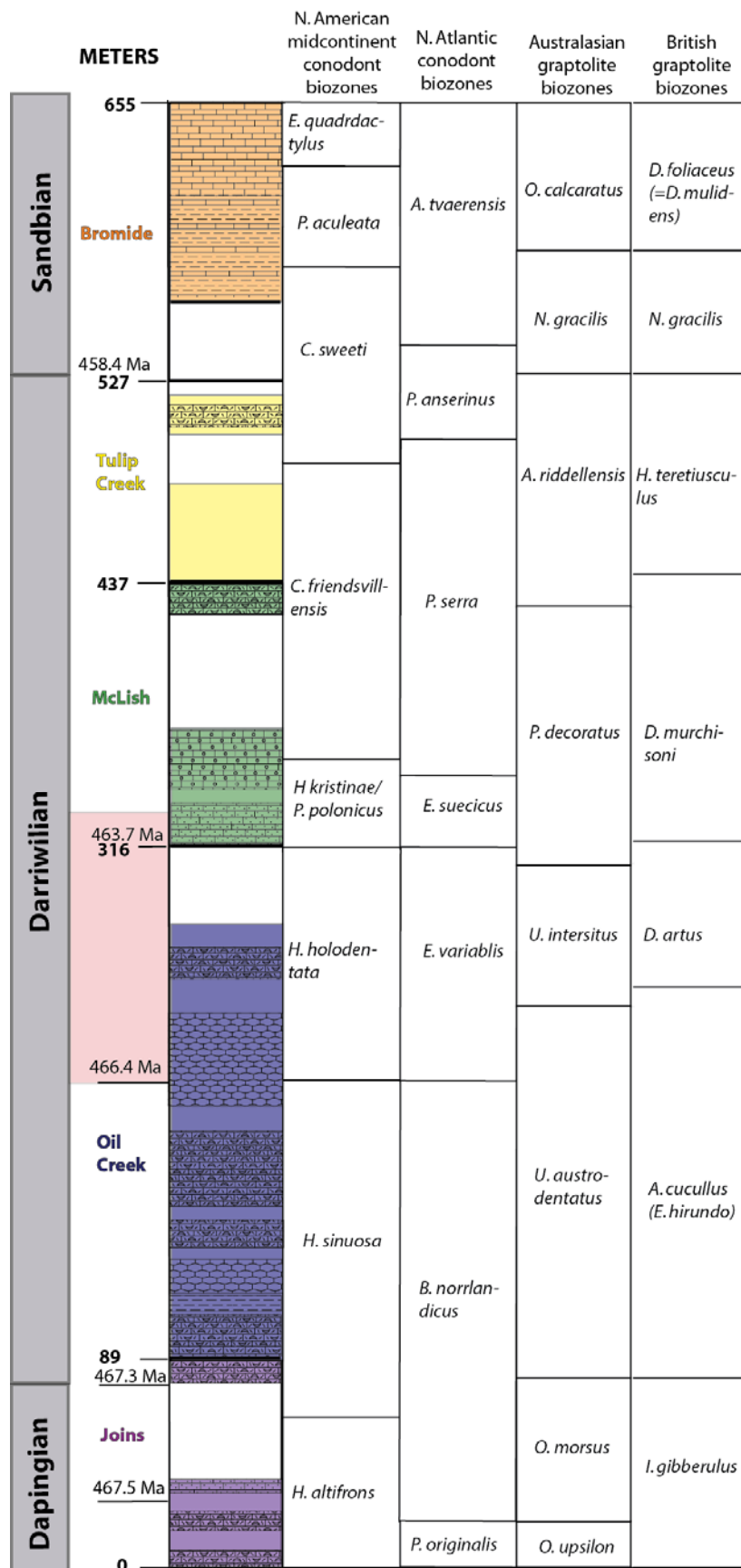


Figure DR1. Chart of measured section of the Simpson Group with biozone correlations and absolute ages.

Colored areas indicate sections measured in the field. Areas shown in white were covered or did not crop out within the field areas. Lithological symbol overlays indicate where high-quality diversity data were obtained and used in analyses. Peach color highlights the interpreted onset of the GOBE in Oklahoma. Total formation thicknesses are based on Fay (1989). Conodont and graptolite zonation for the Simpson Group follows Bauer (1987, 1994, 2010). Correlations follow Cooper and Sadler (2012) and Wang et al. (2013). Absolute ages from Cooper and Sadler (2012).

Part 2. Data analysis

Analyzing diversity and sample bias: Sample size rarefaction and bootstrapping

The vegan package (Oksanen et al., 2015) in R (R Core Team, 2013) was used to compute rarefied species counts and plot collection curves for the ten stratigraphic bins. Table DR1 lists species abundances in each bin. The full dataset includes species abundances in 1-meter stratigraphic context (see Trubovitz, 2016). The vegan function “rarefy” was used to generate rarefied species counts for multiple samples based on Hurlbert’s (1971) equation (Oksanen et al., 2015). Another vegan function, “rrarefy,” was used to generate downsampled matrices from which multiple rarefaction trials were obtained for bootstrapping analyses. Bootstrapping analyses further constrained rarefaction values by generating error estimates for each stratigraphic bin. This method is one of the most widely-used statistical resampling techniques in paleontology (Kowalewski and Novack-Gottshall, 2010). The R package “boot” (Canty and Ripley, 2015; Davidson and Hinkley, 1997) was used in this study as an additional method for defining the uncertainty of rarefied species richness. The function “boot” was used to repeat 10,000 species counts for each bin, based on matrices downsampled to 33 individuals. The mean and standard deviation of these trials were used to estimate error for rarefied diversity levels of each stratigraphic bin.

Rarefaction of 10 stratigraphic bins (309 meters of section) shows a general increase in diversity through time (Fig. 2, Table 1). Bins 1-3 cluster tightly at the bottom of the graph and plot, indicating relatively low diversity. Bin 4 demonstrates intermediate diversity. High diversity is exhibited by steeply arcing curves for Bins 5-10. An alternative binning scheme, including all lower-resolution data (426 meters of section) divided among 9 bins, shows congruent timing of diversity increase. The primary analysis is based on using all 10 stratigraphic bins as shown in Figure 2 and Figure DR2. Rarefaction was also conducted with

bin of the smallest sample size (Bin 6) removed (Figure DR3), which produced congruent results.

When all 10 bins are included, mean species diversity calculated via rarefy for Bins 1-3 is statistically lower than Bins 5-10 (one-tailed T-test, $p=0.004$). Diversity values obtained from the bootstrapped rarefaction analysis closely resembled those calculated by “rarefy” to within ~0.2 species (Fig. 3). Diversity values obtained from bootstrap analyses were significantly higher for Bins 5-10 than for Bins 1-3 (one-tailed T-test, $p < 0.01$). Regardless of whether Bin 4 is included in the high-diversity or low-diversity group, the results remain significant ($p=0.01$ and $p=0.005$, respectively, compared to Bonferroni-adjusted alpha 0.0167).

Similar statistical results are obtained if Bin 6 is excluded: mean species diversity calculated via rarefy for Bins 1-3 is statistically lower than Bins 5, 7-10 (one-tailed T-test, $p=0.001$), and regardless of whether Bin 4 is included in the high-diversity or low-diversity group, the results remain significant ($p < 0.001$ and $p < 0.001$, respectively, compared to Bonferroni-adjusted alpha 0.0167).

Table DR1. Brachiopod species diversity in 10-bin stratigraphic scheme.

Each species is listed in alphabetical order. Numbers indicate the abundance of each species in bins 1-10.

Stratigraphic binning scheme	<i>Anamalorthis oklahomensis</i>	<i>Ancistrothyndia costata</i>	<i>Ancistrothyndia globularis</i>	<i>Ancistrothyndia perplexa</i>	<i>Anthrocrania subquadrata</i>	<i>Atetasma sulcatum</i>	<i>Chaulistomella crassa</i>
Bin 1	31	2	5	0	0	0	0
Bin 2	24	0	0	1	0	0	0
Bin 3	124	0	0	0	0	0	0
Bin 4	69	0	0	1	0	0	0
Bin 5	60	1	0	5	0	0	0
Bin 6	4	0	0	0	0	0	0
Bin 7	0	7	0	12	0	0	0
Bin 8	0	0	0	8	0	3	0
Bin 9	30	0	0	0	0	0	0
Bin 10	0	0	0	0	1	0	6
Totals:	342	10	5	27	1	7	6
Stratigraphic binning scheme	<i>Chaulistomella magna</i>	<i>Chaulistomella mira</i>	<i>Chaulistomella nitens</i>	<i>Chaulistomella obesa</i>	<i>Dactylogonia sculpturata</i>	<i>Desmorthis costata</i>	<i>Desmorthis nevadensis</i>
Bin 1	0	0	0	0	0	35	492
Bin 2	0	0	0	0	0	2	147
Bin 3	0	0	0	0	0	0	69
Bin 4	0	0	0	0	0	0	6
Bin 5	0	1	9	0	0	0	2
Bin 6	0	2	1	1	0	0	1
Bin 7	0	0	0	0	0	2	14
Bin 8	0	0	0	0	0	0	10
Bin 9	1	4	1	0	1	0	0
Bin 10	9	3	3	69	0	0	0
Totals:	10	10	14	70	1	39	741
Stratigraphic binning scheme	<i>Doleroides compressus</i>	<i>Doleroides oklahomensis</i>	<i>Dorytreta bella</i>	<i>Fasifera dalmenelloidea</i>	<i>Glyptorthis costellata</i>	<i>Glyptorthis crenulata</i>	<i>Glyptorthis sp. 4</i>
Bin 1	0	15	2	0	0	0	0
Bin 2	0	0	1	0	0	0	1
Bin 3	0	0	1	0	0	0	0
Bin 4	0	0	0	0	0	0	0
Bin 5	0	0	0	0	0	0	0
Bin 6	0	3	0	0	0	0	0
Bin 7	0	8	1	0	0	0	0
Bin 8	0	0	1	0	0	0	2
Bin 9	1	2	1	0	0	0	0
Bin 10	1	7	1	4	1	11	0
Totals:	2	35	8	4	1	49	3

Stratigraphic binning scheme	Glyptorthis_unicata	Hesperorthis_crinerensis	Hesperorthis_matutina	Hesperorthis_sulcata	Macrocoelia_bella	Mimella_extensa	Mimella_sp._2
Bin 1	0	0	0	12	0	0	0
Bin 2	0	0	0	19	0	0	0
Bin 3	0	0	0	57	0	0	0
Bin 4	0	1	0	50	0	0	1
Bin 5	0	1	0	61	0	0	3
Bin 6	0	0	1	1	0	0	1
Bin 7	0	0	0	117	1	0	0
Bin 8	0	0	0	7	0	0	0
Bin 9	2	1	0	0	1	1	1
Bin 10	0	8	0	0	3	3	5
Totals:	2	11	324	1	4	11	74
Stratigraphic binning scheme	Multicostellata_convexa	Murinella_sp._2	Opikina_expatita	Opikina_extensa	Opikina_formosa	Opikina_gregaria	Orbiculoidea_eximia
Bin 1	0	0	0	0	0	0	0
Bin 2	0	0	0	0	0	0	0
Bin 3	0	0	4	0	0	0	0
Bin 4	0	0	0	0	1	1	1
Bin 5	0	0	0	0	0	0	0
Bin 6	0	0	0	0	0	0	0
Bin 7	0	0	0	0	0	14	0
Bin 8	0	0	0	0	0	0	0
Bin 9	0	0	0	8	2	7	1
Bin 10	1	0	10	10	5	351	5
Totals:	1	4	18	8	373	6	1
Stratigraphic binning scheme	Orthambonites_dinorthis	Orthambonites_minus	Orthambonites_subconvexus	Oxoplectra_oxydentalis	Paurorthis_macrodeltoidea	Platymena?_bellatula	Plectorthis_punctata
Bin 1	16	5	0	0	0	0	0
Bin 2	222	0	2	0	0	0	0
Bin 3	159	2	1	1	0	0	0
Bin 4	34	1	0	0	0	0	0
Bin 5	21	5	3	0	0	0	1
Bin 6	4	2	2	0	0	1	0
Bin 7	16	211	16	0	0	0	0
Bin 8	16	20	0	0	0	0	0
Bin 9	0	3	0	0	0	0	0
Bin 10	0	7	0	1	1	1	1
Totals:	488	256	24	1	1	1	2
Stratigraphic binning scheme	Plectorthis_symmetrica	Protozoya_costata	Psychopleurella_ohaihomani	Rostricellula_cuneata	Rostricellula_parva	Rostricellula_transversa	Skendioloides_ohaihomensis
Bin 1	0	0	0	0	2	0	0
Bin 2	0	0	0	1	1	0	0
Bin 3	0	0	0	0	1	0	0
Bin 4	0	0	0	0	1	0	0
Bin 5	0	0	0	0	1	0	0
Bin 6	0	0	0	0	1	4	0
Bin 7	1	1	0	0	6	0	0
Bin 8	0	0	1	0	0	0	3
Bin 9	0	0	0	1	1	0	0
Bin 10	1	0	0	3	1	0	34
Totals:	2	1	1	5	14	4	37

Stratigraphic binning scheme	Skendioides_perfectus	Sowerbyella_plicatifera	Sowerbyella_veritilis	Sowerbyella_vulgata	Sowerbyites_hamii	Sowerbyites_lamellosus	Sp_10
Bin 1	1	0	0	0	0	0	0
Bin 2	0	0	0	0	0	0	0
Bin 3	0	0	0	1	0	0	0
Bin 4	0	0	0	0	1	0	0
Bin 5	0	3	3	2	3	0	0
Bin 6	0	0	0	0	0	0	0
Bin 7	1	0	0	0	0	0	0
Bin 8	1	0	0	0	0	0	0
Bin 9	1	19	48	451	4	12	0
Bin 10	9	27	9	35	0	0	17
Totals:	13	49	60	490	4	12	17
Stratigraphic binning scheme	Sp_3	Sp_5	Sp_8	Sp_Unknown_1_Bromide_M	Sp_Unknown_1_Oil_Creek	Sp_Unknown_1_McLish	Sp_Unknown_2_Bromide_M
Bin 1	1	1	0	0	0	0	0
Bin 2	0	0	0	0	7	0	0
Bin 3	0	0	0	0	1	0	0
Bin 4	0	1	0	0	3	0	0
Bin 5	0	0	0	0	0	0	0
Bin 6	0	0	0	0	0	0	0
Bin 7	0	1	6	0	0	0	0
Bin 8	0	1	0	0	0	0	0
Bin 9	0	0	0	1	0	2	1
Bin 10	0	0	0	1	0	0	1
Totals:	1	4	6	2	11	2	2
Stratigraphic binning scheme	Sp_Unknown_2_Oil_Creek	Sp_Unknown_3_Oil_Creek	Sp_Unknown_Bromide_Inar	Sphenotreta_sulcata	Strophomena_costellata	Strophomena_criniferensis	Strophomena_oklahomensis
Bin 1	0	0	0	3	0	0	0
Bin 2	3	2	0	1	1	0	0
Bin 3	0	0	0	1	0	0	0
Bin 4	0	0	0	0	1	0	0
Bin 5	0	0	0	1	0	0	0
Bin 6	0	0	0	0	3	0	2
Bin 7	0	0	0	10	13	0	2
Bin 8	0	0	0	8	5	0	1
Bin 9	0	0	1	0	16	1	5
Bin 10	0	0	0	0	101	0	40
Totals:	3	2	1	24	140	1	50
Stratigraphic binning scheme	Valcouria_deckeri	Valcouria_tenuis	Valcouria_transversa	Totals per bin			
Bin 1	0	0	0	623			
Bin 2	0	2	0	442			
Bin 3	1	1	0	431			
Bin 4	0	0	0	193			
Bin 5	0	1	0	204			
Bin 6	2	0	0	33			
Bin 7	6	0	0	469			
Bin 8	6	1	0	102			
Bin 9	4	11	25	710			
Bin 10	0	0	1	808			
Totals:	19	16	26	4015			

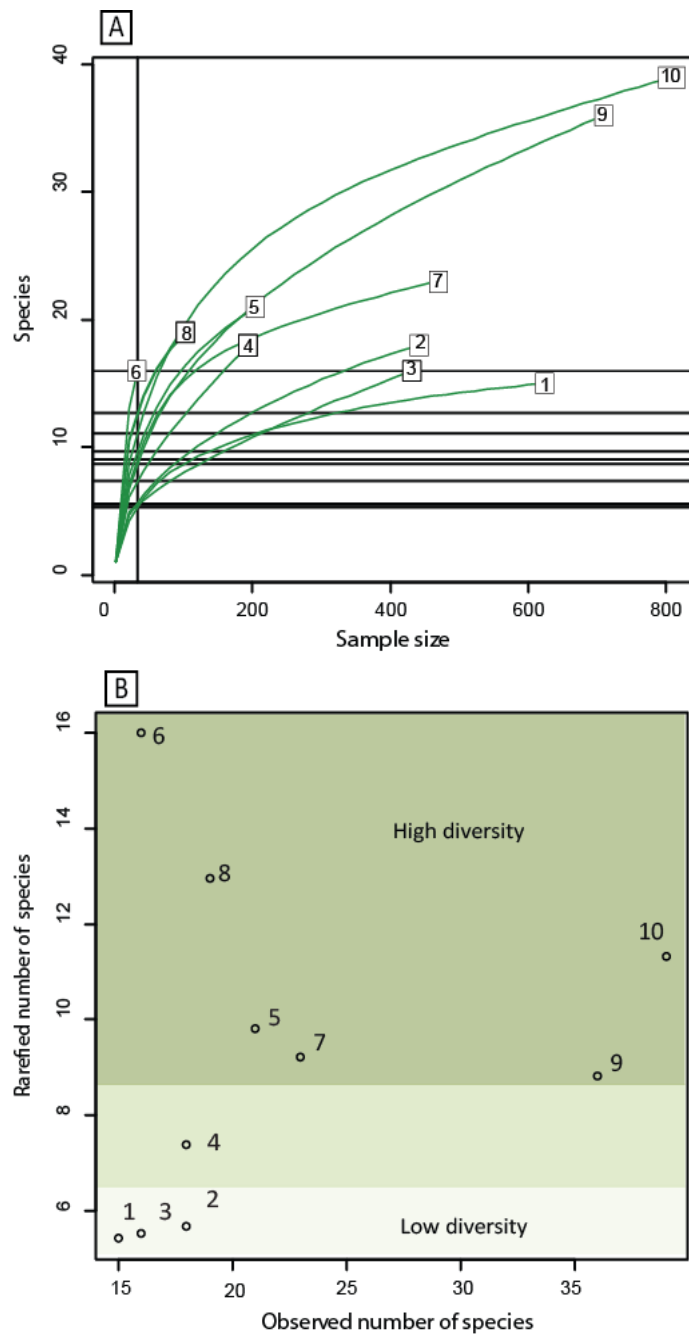


Figure DR2. Rarefaction for diversity based on ten stratigraphic bins.

(A) Collection curves for each stratigraphic bin. Rarefaction is based on smallest sample (Bin 6).

(B) Plot comparing the observed number of species and rarefied number of species in each bin. The vertical line in (A) represents minimum sample size (33 individuals), where the curves have been spliced and plotted for direct comparison of diversity levels in (B).

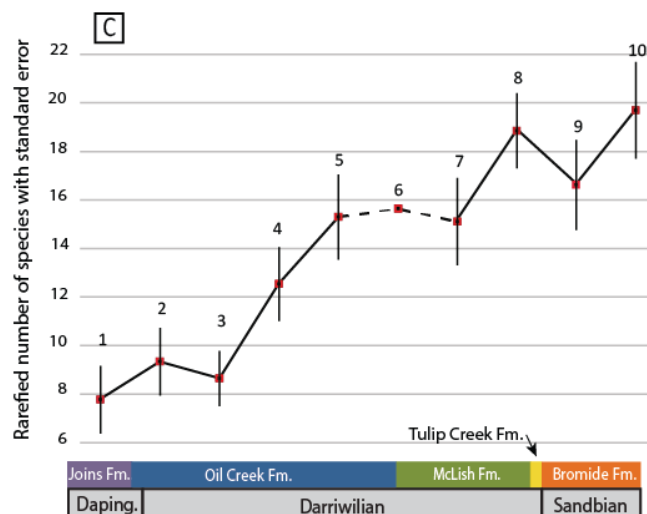
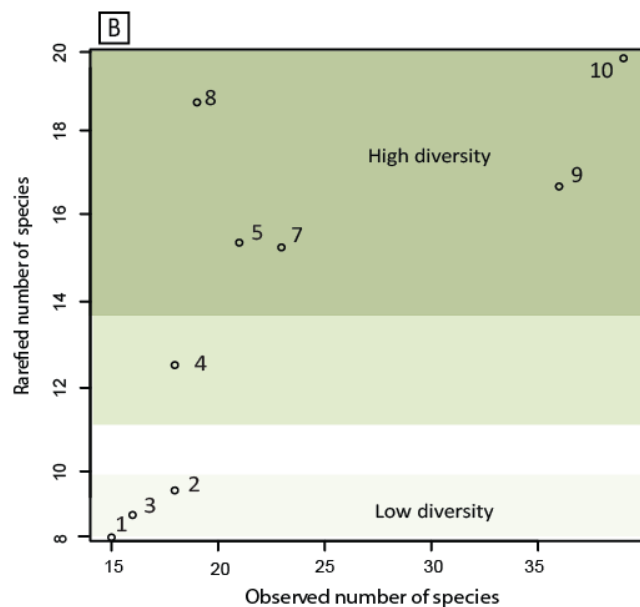
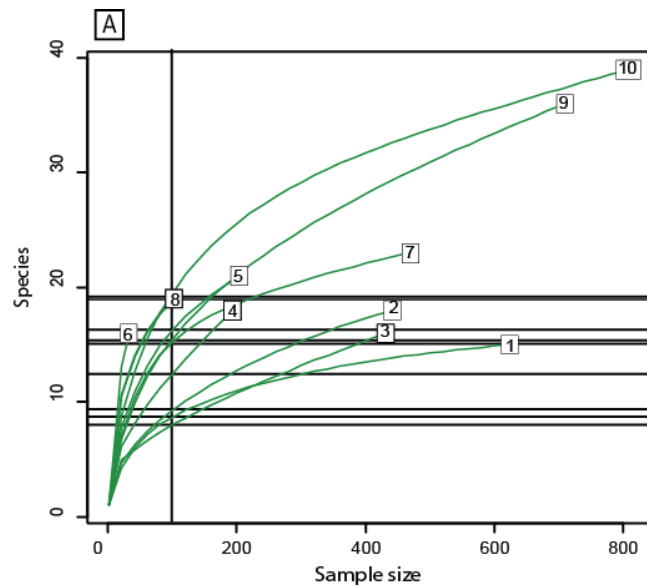


Figure DR3. Rarefaction for diversity based on ten stratigraphic bins.

(A) Collection curves for each stratigraphic bin. Rarefaction is based on smallest sample (Bin 8) after excluding Bin 6.

(B) Plot comparing the observed number of species and rarefied number of species in each bin. The vertical line in (A) represents minimum sample size (102 individuals), where the curves have been spliced and plotted for direct comparison of diversity levels in (B).

(C) Rarefaction curves sliced through minimum sample size (102 individuals; vertical line in A) and plotted temporally (Dapin. = Dapingian). Bin 6 is plotted using the observed number of species.

Calculation:	Bin 1	Bin 2	Bin 3	Bin 4	Bin 5	Bin 6	Bin 7	Bin 8	Bin 9	Bin 10
Rarefied Species	5.41	5.68	5.53	7.39	9.80	16.00	9.21	12.96	8.82	11.33
Standard Error	1.32	1.32	1.08	1.44	1.65	0.00	1.70	1.46	1.75	1.89

Table DR2. Rarefaction calculations for diversity in each stratigraphic bin.

The rarefied species numbers for each bin and associated standard error were calculated using the “rarefy” function in the R package “vegan.”

Calculation:	Bin 1	Bin 2	Bin 3	Bin 4	Bin 5	Bin 6	Bin 7	Bin 8	Bin 9	Bin 10
Mean rarefied species (10,000 trials)	5.4	5.7	5.5	7.4	9.8	16.0	9.2	13.0	8.9	11.3
Standard deviation among trials	1.3	1.3	1.1	1.4	1.6	0.0	1.7	1.5	1.8	1.9

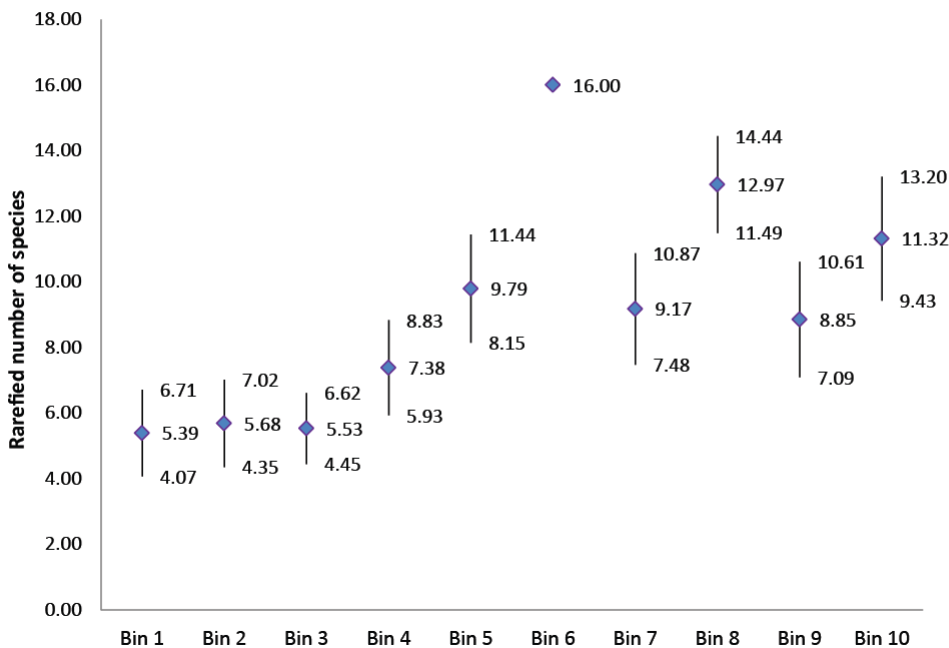


Figure DR3. Bootstrapped rarefaction results.

Blue diamonds indicate the mean rarefied species values with 10,000 repeated trials. Numbers above and below the diamonds and correlating line segments are the values within one standard deviation of the mean. These results are congruent with the results of the “rarefy” results, in that the highest probable values for bins 1-3 do not overlap with the lowest probable values for bins 5-10.

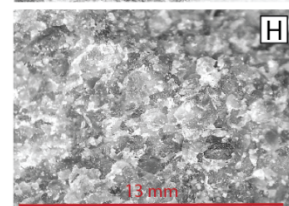
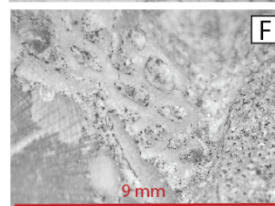
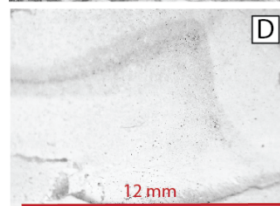
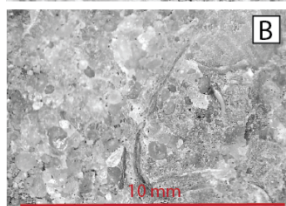
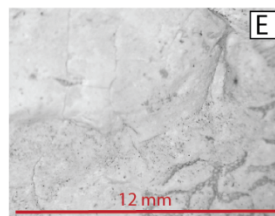
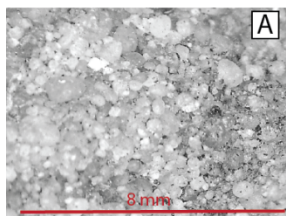
Analyzing facies bias: facies rarefaction

Rarefaction based on facies type was also performed to test whether diversity trends were impacted by facies type. Bins were constructed for each of the 10 most common facies types in the section: crystalline grainstone, packstone, sandy grainstone, grainstone, thin-bedded alternating limestone and shale, cover, shale, sandstone, micritic mudstone, and wackestone (Table DR3). Carbonate facies types are based on matrix:grain ratios from Dunham's classification of limestones (1962). Seven facies types were fossiliferous: crystalline limestone (1), thin-bedded alternating limestone and shale (2), packstone (3), grainstone (4), micritic mudstone (5), wackestone (6), and sandy grainstone (7).

Table DR3. Descriptions the ten generalized Simpson Group facies used in this study.

Carbonate facies are based on Dunham (1962). Textural photos represent (A) sandstone, (B) sandy grainstone, (C) shale, (D) micritic mudstone, (E) wackestone, (F) packstone, (G) grainstone, and (H) crystalline grainstone.

<u>Distinguishable depositional texture</u>								<u>Texture indistinguishable</u>	
Contains Sand		Contains carbonate mud				Multiple depositional textures	Contains skeletal grains, unit in-situ	Lithology uncertain, unit out-of-place	
< 10% skeletal grains	>10% skeletal grains	> 90% clay, laminated & fissile	Matrix-supported		Grain-supported				
			<10% skeletal grains	>10% skeletal grains	> 50% grains				Lacks mud
							Lime and shale beds 1mm-10cm		
Sandstone	Sandy grainstone	Shale	Micritic mudstone	Wackestone	Packstone	Grainstone	Alternating limestone and shale	Crystalline grainstone	Cover



All 309 meters of section were grouped by facies category, irrespective of formation and stratigraphic positioning (see Trubovitz, 2016). With a lithological rather than stratigraphic binning scheme, facies biases could be directly measured using rarefaction in the vegan package (Oksanen et al., 2015).

Results of the facies rarefaction analysis indicates that species diversity is similar in most lithologies (Fig. 4, Table 4). Six facies share overlapping rarefaction curves and standard error bars (Fig. 5) which indicate similar diversity potentials at similar sampling size. Sandy grainstone, however, is characterized by lower species diversity. Thus, all fossiliferous facies except sandy grainstone are likely to demonstrate similar diversity at similar sampling intensity.

Table DR4. Rarefaction calculations for diversity in each facies bin.

The rarefied species numbers for each facies and associated standard error were calculated using the “rarefy” function in the R package “vegan.”

Calculation	Crystalline	Alternating	Packstone	Grainstone	Mudstone	Wackestone	Sandy grainstone
Rarefied speices	21.49	21.47	23.84	23.37	23	21.63	12.78
Standard error	2.37	2.3	1.66	2.02	0	2.05	0.45

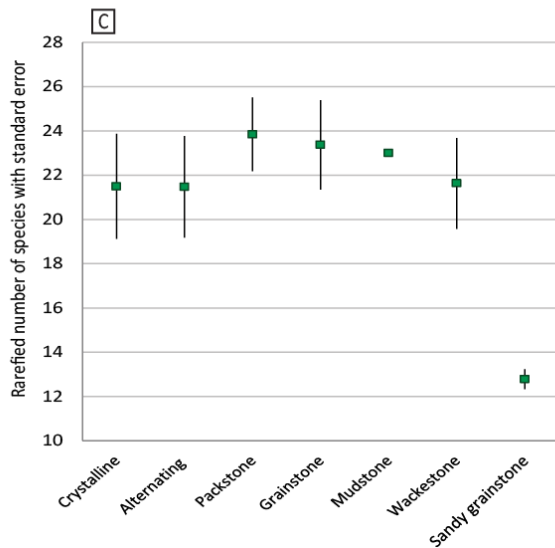
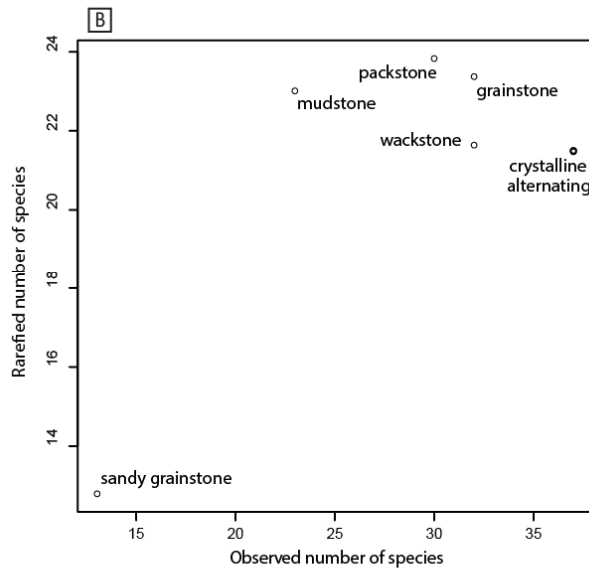
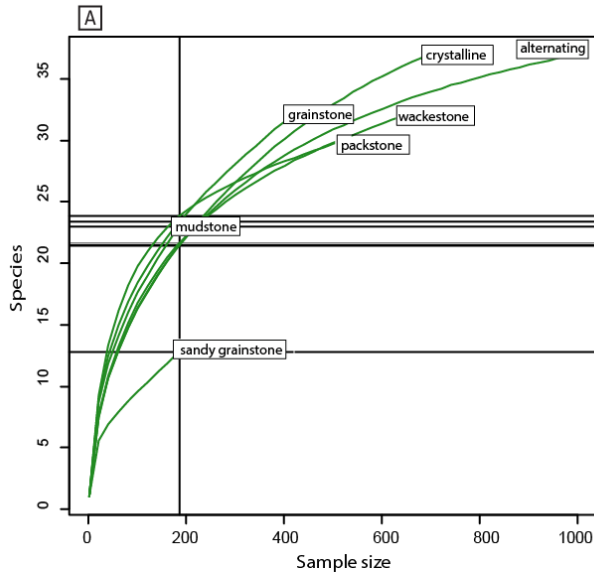


Figure DR4. Rarefaction for diversity based on facies type.

(A) Collection curves for the seven fossiliferous facies types;

(B) Plotted rarefied diversity for each facies compared to observed number of species. The vertical line in (A) represents minimum sample size (186 individuals), where the curves have been spliced and plotted for direct comparison of diversity levels in (B).

(C) Plot of rarefied species diversity for each facies type with standard error bars for each calculation.

The potential impact of facies bias was also assessed using the Fisher's Exact Test (Fisher, 1929) to examine whether adjacent stratigraphic bins exhibited statistically different facies distributions. For example, if a set of facies types exhibit different diversity contents on rarefaction curves, it is important to determine the extent to which stratigraphic compositions of the bins are similar. Therefore, Fisher's Exact Test was used to find the likelihood of stratigraphic bins exhibiting similar diversity based on facies composition alone.

Fisher's Exact Test was used to examine facies distribution between the temporal intervals that exhibited highest diversity increase in the species rarefaction. This tests whether the observed diversity increase is attributable to facies differences between bins. No significant differences in occur between Bins 3 and 4 ($p = 0.36$) or Bins 3 and 5 ($p=0.11$). Notably, the lower diversity sandy grainstone comprises very little of these bins. Thus, the three bins would be expected to yield the similar levels of brachiopod diversity at congruent sampling intensities.

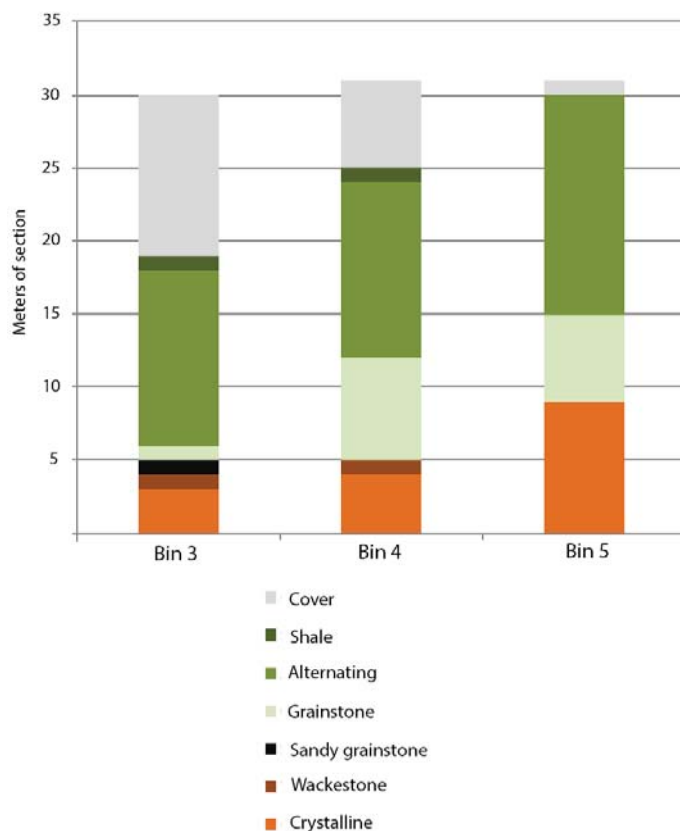


Figure DR5. Stacked facies composition of stratigraphic bins 3-5: the record at the onset of the GOBE in Oklahoma.

All three bins are dominated by thin-bedded alternating limestone and shale facies. They also contain relatively large amounts of crystalline grainstone. Bin 3 deviates slightly from the other two bins in that it contains one meter of sandy grainstone and relatively less grainstone. However, these differences were not statistically significant.

Analyzing environmental gradient bias: Cross-basin comparison

Data from the Bromide Formation (Early Sandbian) along I-35 and Highway 177 were used to test for difference in diversity levels along two points of the basin's depth gradient. Synchronous deposition occurred 16 kilometers apart at relatively different positions along the ramp, yet both sections yield similar diversity levels. Rarefaction of I-35 and Highway 177 samples of the Bromide Formation indicate down-sampled species richness of 46.00 and 47.90, respectively. Both curves follow similar upward-curving trajectories that begin to flatten at the minimum sample size of 1479 (Fig. 6). Throughout the collection curve arcs, the Highway 177 sections exhibit slightly higher diversity than the I-35 sections. However, this difference never surpasses more than a few species.

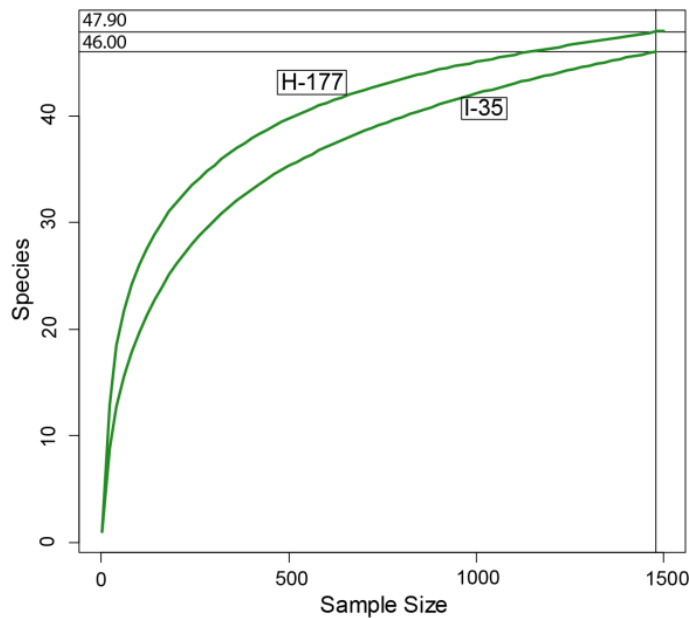


Figure DR1. Rarefaction curves for Bromide Formation sections at I-35 and Hwy 177.

Curves indicate the expected number of taxa collected from a given sample size. Rarefied numbers at the minimum sample size (1479) are 47.90 and 46.00 for 177 and I-35, respectively.

Facies types within the two sections were also compared, to determine whether different positions along the ramp presented measurably different environments to the fauna. Comparing normalized sections, the Bromide Formation section at Highway 177 includes a higher proportion of facies characteristic of shallow water environments than the I-35 section (Fig. 7). Sandy grainstone and mud-rich carbonates comprise the most common deposits upramp; whereas the downramp section has a greater proportion of muddy carbonates and no sandy layers are fossiliferous. The overall facies distributions of the two sections are significantly different (Fisher's Exact Test for independent distributions, $p < 0.05$). In addition, when sandy and non-sandy facies proportions are compared in a 2x2 contingency matrix, the Fisher's Exact Test returns a p-value of 0.03. This indicates that the proportion of siliciclastic sediment is significantly higher along Highway 177, consistent with prior interpretations that the Bromide section on Highway 177 is upramp of the Bromide section on I-35 (Carlucci et al., 2014; Ham, 1973; Longman, 1982).

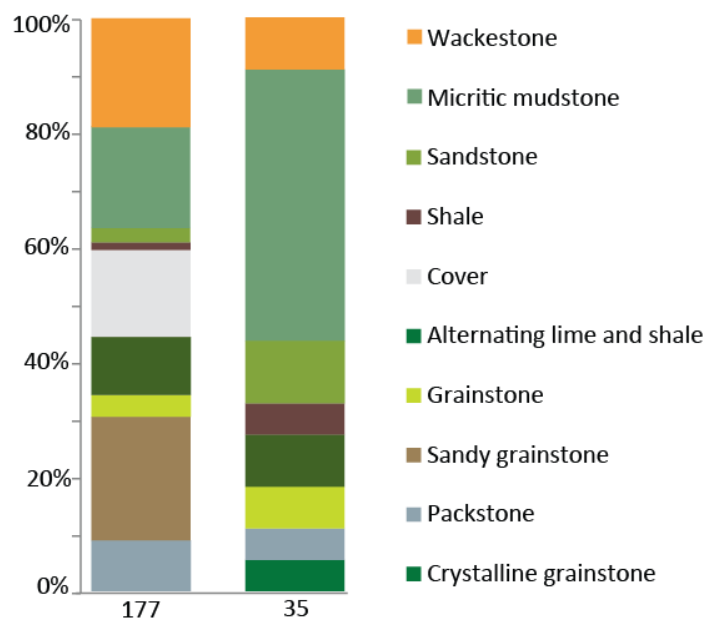


Figure DR7. Facies composition of Bromide Formation sections at I-35 and Hwy 177 localities.

Compositions are normalized to 100%, and based on definitions from Table 1.



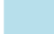
Geographic occurrences of Simpson Group brachiopods

Many Simpson Group brachiopod genera also occur in other geographic areas, with first occurrences ranging from the Cambrian Period to Early Sandbian Stage (*Treatise of Invertebrate Paleontology* (Kaesler, 1997) and the Paleobiology Database (www.paleodb.org); Table DR5). Of the 32 genera observed in the Simpson Group, one was first recorded in the Cambrian, 13 from the Arenig (Floian-Early Darriwilian), 10 from the Llanvirn (Middle-End Darriwilian), seven from the Caradoc (Early Sandbian-Middle Katian), and one known to the Ordovician but with uncertain first stratigraphic occurrence. Geographic distribution comparisons were made with Baltica and South China as these two paleoplates have more complete brachiopod diversity data than other plates. Six Simpson Group genera have not been found on South China or Baltica (Table 5), and three of these are endemic to Laurentia. However, most brachiopods, particularly those appearing in the upper Simpson Group sections, are widespread genera. Six occur in China but not Baltica, four in Baltica but not China, and 16 occur in at least these three locations. Thus, nearly 90% of Simpson Group genera are found on at least one continent other than Laurentia (Table DR5). The extremely limited endemism of Simpson Group brachiopods at the genus level indicates that dispersal was an important mechanism during the Middle Ordovician diversification.

Table DR5. Geographic occurrences of Simpson Group genera

This table lists the occurrences of genera observed in the Simpson Group of Oklahoma. Occurrences in other regions are based on information from the *Treatise on Invertebrate Paleontology* (Kaesler, 1997) and the Paleobiology Database (www.paleodb.org, accessed February, 2016). Age of first occurrence is noted, but there are no data for the relative timing of appearance on each paleocontinent. Thus, the color code reflects the entire documented history of a genus' occurrence, rather than an isolated interval of interest.

Genus	Origin: occurrence(s)
<i>Acanthocrania</i>	Caradoc: USA, UK, Norway, Ireland, China
<i>Anomalorthis</i>	Arenig: USA
<i>Ancistrorhyncha</i>	Llanvirn: N America, Baltic, Kazakhstan, Central Asia, Eastern Siberia, China
<i>Atelelasma</i>	Llanvirn: USA
<i>Chaulistomella</i>	Caradoc: N America, Scotland, Siberia, Kirghizia
<i>Dactylogonia</i>	Caradoc: N America, Europe
<i>Desmorthis</i>	Arenig: N America, England, Bolivia, SW China, Argentina
<i>Doleroides</i>	Caradoc: N America, Scotland, Ireland, Kazakhstan, Australia, W China, Tibet
<i>Dorytreta</i>	Llanvirn: N America, Eastern Siberia, Kazakhstan, China, Norway
<i>Fasifera</i>	Caradoc: N America
<i>Glyptorthis</i>	Arenig: China, N America, Iran, Bolivia, Czech Republic, Norway, Argentina
<i>Hesperorthis</i>	Arenig: cosmopolitan
<i>Macrocoelia (Colaptomena)</i>	Llanvirn: N America, Europe, Peru
<i>Mimella</i>	Arenig: China, USA, UK, Russia, Argentina
<i>Multicostella</i>	Arenig: USA, UK, Russia, Canada
<i>Murinella</i>	Llanvirn: N America, Australia, Russia, UK
<i>Oepikina</i>	Llanvirn: N America, Baltic, China, Australia, Sweden, UK, Mongolia
<i>Orbiculoidea</i>	Ordovician: cosmopolitan
<i>Orthambonites</i>	Arenig: Baltoscandia, Russia, Argentina, China, N America, Europe
<i>Oxoplectra</i>	Llanvirn: N America, Eurasia, China
<i>Paurorthis</i>	Cambrian: cosmopolitan
<i>Platymena</i>	Caradoc: N America, Kazakhstan, Russia, Australia
<i>Plectorthis</i>	Arenig: China, Morocco, Australia, N America, Europe
<i>Protozyga</i>	Caradoc: cosmopolitan
<i>Ptycopleurella</i>	Llanvirn: cosmopolitan
<i>Rostricellula</i>	Llanvirn: N America, Europe, Asia, S America, Middle East, Russia
<i>Skenidiodes</i>	Arenig: cosmopolitan
<i>Sowerbyella</i>	Arenig: cosmopolitan
<i>Sowerbyites</i>	Arenig: N America, Ireland, Mongolia, Australia, China
<i>Sphenotreta</i>	Llanvirn: N America, Siberia, UK
<i>Strophomena</i>	Arenig: N America, Europe, China
<i>Valcouria</i>	Arenig: N America, Scotland, Norway, NE China, Central Asia, South America

 = not found on Baltica or S. China
 = not found on S. China
 = not found on Baltica

REFERENCES CITED

- Bauer, J.A., 1987, Conodonts and conodont biostratigraphy of the McLish and Tulip Creek Formations (Middle Ordovician) of south-central Oklahoma: Oklahoma Geological Survey Bulletin 141, 58 p.
- Bauer, J.A., 1994, Conodonts from the Bromide Formation (Middle Ordovician), south-central Oklahoma: *Journal of Paleontology*, v. 68, p. 358-376.
- Bauer, J.A., 2010, Conodonts and conodont biostratigraphy of the Joins and Oil Creek Formations, Arbuckle Mountains, South-Central Oklahoma. Oklahoma Geological Survey Bulletin 150, 44 p.
- Canty, A., and Ripley, B., 2016, boot: Bootstrap R (S-Plus) Functions. R package version 1.3-15.
- Carlucci, J.R., Westrop, S.R., Brett, C.E., and Burkhalter, R., 2014, Facies architecture and sequence stratigraphy of the Ordovician Bromide Formation (Oklahoma): a new perspective on a mixed carbonate-siliciclastic ramp: *Facies*, v. 60, p. 987-1012.
- Cooper, R.A., and Sadler, P.M., 2012, The Ordovician Period: *in* Gradstein, F.M., Ogg, J.G., Schimtz, M.D., and Ogg, G.M., eds., *The Geologic Time Scale 2012*: Amsterdam, Elsevier, p. 489–523.
- Davison, A.C., and Hinkley, D.V., 1997, *Bootstrap methods and their applications*: Cambridge, Cambridge University Press, 582 p.
- Dunham, R.J., 1962, Classification of carbonate rocks according to depositional texture: *Classification of Carbonate Rocks: in* Hamm, W.E., ed., *Classification of Carbonate Rocks, A Symposium*. American Association of Petroleum Geologists, p. 108-121.

- Fisher, R.A., 1929, Tests of significance in harmonic analysis: Proceedings of the Royal Society of London. Series A, v. 125, p. 54-59.
- Ham, W.E., and Amsden, T.W., 1973, Regional geology of the Arbuckle Mountains, Oklahoma: Oklahoma Geological Survey Special Publication 73-3, 61 p.
- Hurlbert, S.H., 1971, The nonconcept of species diversity: a critique and alternative parameters: Ecology, v. 52, p. 577-586.
- Kaesler, R., ed. 1997. Treatise on Invertebrate Paleontology, Part H: Brachiopoda, Revised: Boulder, Colorado, Geological Society of America (and University of Kansas Press).
- Kowalewski, M., and Novack-Gottshall, P.M., 2010, Resampling methods in paleontology: Paleontological Society Papers, v. 16, p. 19-54.
- Longman, M.K., 1982, Depositional setting and regional characteristics, *in* Sprinkle, J., ed, 1982. Echinoderm faunas from the Bromide Formation (Middle Ordovician) of Oklahoma. The Kansas University Paleontological Institute, p. 6-11.
- Oksanen, J.F., Blanchet, F.G., Kindt, R., Legendre, P., Minchin, P.R., O'Hara, R.B., Simpson, G.L., Solymos, P., Stevens, M.H.H., NS Wagner, H., 2015, Vegan: Community Ecology Package. R package version 2.2-1.
- R Core Team, 2013. R: A language and environment for statistical computing: R Foundation for Statistical Computing, Vienna, Austria.
- Trubovitz, S., 2016, Reconstructing the Great Ordovician Biodiversification Event through brachiopods of Oklahoma [M.S. thesis]: Athens, Ohio University, 209 p.

Wang, Z.H., Bergström, S.M., Zhen, Y.Y., Chen, X., Zhang, Y.D., 2013, On the integration of Ordovician conodont and graptolite biostratigraphy: new examples from Gansu and Inner Mongolia in China: *Alcheringa*, v. 37, p. 510-528.